10298 *Biochemistry* **2009,** *48,* 10298–10307
DOI: 10.1021/bi900123j

BIOCHEMISTRY
including biophysical chemistry & molecular biology
Article

Structure Elucidation and Preliminary Assessment of Hydrolase Activity of PqsE, the *Pseudomonas* Quinolone Signal (PQS) Response Protein‡

Shen Yu,§ Vanessa Jensen,∥ Janine Seeliger,⊥ Ingo Feldmann,# Stefan Weber,△ Erik Schleicher,△ Susanne Häussler,∥ and Wulf Blankenfeldt*,§

§*Department of Physical Biochemistry, Max-Planck-Institute of Molecular Physiology, 44227 Dortmund, Germany,* ∥*Helmholtz Center for Infection Research, 38124 Braunschweig, Germany,* ⊥*Faculty of Chemistry, Technical University of Dortmund, 44227 Dortmund, Germany,* #*Institute for Analytical Sciences, 44139 Dortmund, Germany, and* △*Institute of Physical Chemistry, Albert Ludwigs University of Freiburg, 79104 Freiburg, Germany*

Received December 15, 2008; Revised Manuscript Received September 11, 2009

ABSTRACT: In bacteria, the transcription of virulence genes is usually controlled by a cell density-dependent process known as "quorum sensing" (QS). QS relies on small diffusible signaling molecules that cross the bacterial cell wall and activate target transcription factors after a threshold concentration has been reached. Besides two hierarchical QS circuits based on *N*-acylhomoserine lactones, the human opportunistic pathogen *Pseudomonas aeruginosa* integrates a signaling system that depends on 2-heptyl-3-hydroxy-4-quinolone, termed "*Pseudomonas* quinolone signal" (PQS). PQS is produced from genes encoded in the *pqs* operon, which in addition to the biosynthetic enzymes PqsA−D contains a fifth gene, *pqsE*, that is not required for production of PQS but whose disruption leads to loss of signal transduction in several but not all *pqs* operon-dependent processes. PqsE was hence termed "PQS response protein", but its exact mechanism of action is unknown. We have determined the crystal structure of recombinant PqsE and show that it possesses a metallo-β-lactamase fold with an Fe(II)Fe(III) center in the active site. A copurified ligand was assigned as benzoate and may indicate that PqsE exerts its regulatory effect by converting a chorismate-derived molecule. Further, PqsE was found to slowly hydrolyze phosphodiesters including single- and double-stranded DNA as well as mRNA and also the thioester *S*-(4-nitrobenzoyl)mercaptoethane. Higher activity was observed after incubation with Co^{2+} and, to lesser entent, Mn^{2+}, suggesting that the Fe(II)Fe(III) center of recombinant PqsE may be an artifact of heterologous expression. A crystal complex of the E182A mutant with bis-pNPP was obtained and suggests a catalytic mechanism for hydrolysis.

Pseudomonas aeruginosa is a ubiquitous opportunistic bacterial pathogen that infects a broad range of host organisms. In humans, the bacterium is primarily a nosocomial strain and a serious problem in immuno-compromised patients, such as those with burn wounds or cystic fibrosis, where it is the leading cause of early mortality (*1*). *P. aeruginosa* produces a large arsenal of virulence factors, including extracellular proteases or small molecule toxins like the blue phenazine derivative pyocyanin, to overcome cellular defenses of the host (*2*). Once established in the host, it embeds itself in biofilms, making infections difficult to eradicate (*3*). It is well documented that the biosynthesis of virulence factors and generation of biofilm in *P. aeruginosa* are under quorum sensing (QS)[1] control (*4*, *5*), a signal transduction mechanism involving the production of freely diffusible small "autoinducer" molecules that bind and activate their cognate regulatory proteins after a threshold concentration has been reached. Since these autoinducers also trigger their own production, a positive feedback loop is created that shifts metabolic energy from reproduction to secondary metabolism, thereby ensuring that these processes are only initiated once a certain cell density has been reached (*6*).

In Gram-negative bacteria, QS often utilizes *N*-acylhomoserine lactones (AHLs) as autoinducers, and *P. aeruginosa* employs two AHL-based circuits with autoinducer synthase LasI and its cognate transcription factor LasR, or RhlI and RhlR, respectively. LasRI and RhlRI are arranged in a hierarchical manner with the former controlling the latter. It was, however, found that disruption of *lasR* does not completely abolish the induction of genes that were believed to be controlled by HSLs. This led to the discovery of a signaling system that depends on 2-heptyl-3-hydroxy-4-quinolone, termed the "*Pseudomonas* quinolone signal" PQS (Figure 1), disruption of which also results in loss of the production of several virulence factors (*7*, *8*). Functional studies place PQS in between the Las-Rhl hierarchy (*9*). PQS is first synthesized as 2-heptyl-4-quinolone (HHQ) from anthranilate and an activated β-keto fatty acid by action of the enzymes PqsA-D of the *pqs* operon (*10*−*13*). HHQ is already active as a signaling molecule (*14*), but in *P. aeruginosa*, it gets further modified by PqsH, which is located outside of the *pqs* operon and under control of the LasRI system (*10*). The transcription factor that responds to HHQ and PQS is PqsR (also termed MvfR), encoded slightly downstream of the *pqs* operon. Since PqsR also controls the *pqs* operon itself, PQS indeed functions similarly to other

‡Coordinates and structure factors have been deposited in the Protein Data Bank as entries 2Q0I, 2Q0J, and 3DH8.

*Corresponding author. Tel: +49 231 133 2364. Fax: +49 231 133 2399. E-mail: wulf.blankenfeldt@mpi-dortmund.mpg.de.

[1]Abbreviations: AHL, *N*-acylhomoserine lactone; bis-pNPP, bis-(*p*-nitrophenyl) phosphate; CoA, coenzyme A; EPR, electron paramagnetic resonance; HHQ, 2-heptyl-4-quinolone; ICP-MS, inductively coupled plasma mass spectrometry; PQS, *Pseudomonas* quinolone signal; QS, quorum sensing; S-(4NB)-ME, *S*-(4-nitrobenzoyl)-mercaptoethane; TB, terrific broth.

 Published on Web 09/29/2009

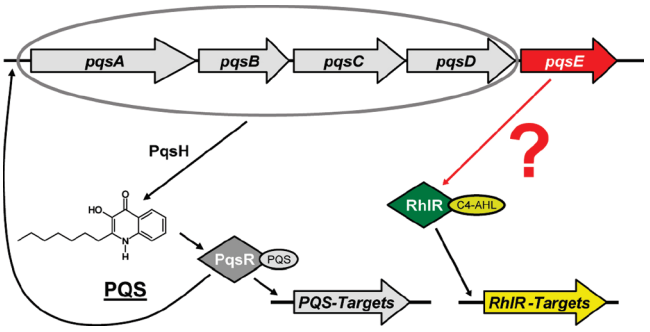

FIGURE 1: Current understanding of the PQS system. C4-AHL (*N*-butyryl-L-homoserine lactone) is the autoinducer of the RhlRI system.

autoinducer molecules (*14*, *15*). PQS may, however, also have additional functions. For example, it has recently been suggested that PQS acts as an iron scavenger that traps iron at the cell surface, from where it can be taken up by other siderophore systems of *P. aeruginosa* (*16*). New data also indicate that PQS is involved in the formation of bacterial membrane vesicles, which package the signaling molecule and thereby increase its solubility (*17*, *18*).

In addition to the biosynthetic enzymes PqsA−D, the *pqs* operon contains a fifth gene, *pqsE* (*10*), which does not take part in the biosynthesis of PQS but whose disruption leads to loss of signal transduction in several but not all processes believed to depend on PQS (*16*). PqsE was hence termed "PQS response protein". The protein was predicted to be cytoplasmatic and to possess a metallo-β-lactamase fold, and Farrow et al. have recently shown that PqsE acts independently of PQS itself by interfering with the AHL-dependent QS transcription factor RhlR through an unknown mechanism (*19*). Even with this new insight, however, the exact molecular function of PqsE still remains enigmatic (Figure 1). Since PqsE controls the expression of important virulence factors like elastase and pyocyanin in *P. aeruginosa* and possibly also functions in a number of other pathogenic bacterial species (*8*, *20*, *21*), PqsE may be an attractive target for therapeutic intervention. We have therefore set out to determine the crystal structure and identify the enzymatic activity of PqsE.

EXPERIMENTAL PROCEDURES

Protein Expression and Purification. *pqsE* was amplified by PCR from *P. aeruginosa* PAO1 genomic DNA with primers pqsE-for (5′-TGAACCGCATATGTTGAGGCTTTC-3′) and pqsE-rev (5′-AATGGGGATCCCTTATCAGTCCAGAGG-CAG-3′) and cloned into the *Nde*I and *Bam*HI sites of pET28a (Merck Biosciences). The resulting plasmid produces PqsE with an N-terminal His_6 tag that can be removed by thrombin cleavage. The plasmid was single-pass sequenced and then transformed into *Escherichia coli* Rosetta pLysS [DE3] (Merck Biosciences). Cells where grown in terrific broth (TB) and then induced with 0.6 mM IPTG for 20 h at 20 °C. Recombinant PqsE was first purified by Ni-NTA affinity chromatography followed by dialysis/thrombin cleavage and then gel filtration in 20 mM Tris-HCl, pH 8.0, and 150 mM NaCl. Purified protein was concentrated to ~20 mg/mL for crystallization and functional assays. Seleno-L-methionine was incorporated by suppressing methionine biosynthesis in LeMaster media (*22*), using BL21-(DE3) pLysS cells. Mutations were introduced with the Quik-Change II XL system (Stratagene). GST, MBP, and Strep-tag II fusion proteins were generated by digesting the pET28a-*pqsE* expression plasmid with *Nde*I and *Xho*I and subcloning the insert into the same sites of expression plasmids delivering the respective fusion proteins, which were purified using their respective affinity tags.

Crystallization. All crystallization experiments were carried out at 20 °C with protein produced from pET28a-*pqsE* after removal of the His_6 tag with thrombin. Initial conditions were determined with Crystal Screen and Crystal Screen 2 (Hampton Research) and then optimized with the hanging-drop method. Diffraction quality crystals were obtained at a protein concentration of 21 mg/mL and a reservoir consisting of 100 mM HEPES, pH 7.6, 200 mM $MgCl_2$, and 28−32% (w/v) PEG 400 (crystal form 1). Crystals begin to decay after 3 days, and it was also important to use freshly prepared protein for crystallization. Crystals of the selenomethionine-labeled protein and of the E182A mutant were obtained under similar conditions. A complex of the E182A mutant with bis-pNPP was prepared by overnight soaking in mother liquor supplemented with 5 mM ligand.

A second crystal form was generated with 0.1 M imidazole, pH 6.5, and 0.6 M NaOAc (crystal form 2). For diffraction data collection, these crystals needed to be cryoprotected, which was achieved by quick washing in reservoir solution supplemented with 15% (v/v) glycerol.

Diffraction Data Collection and Processing. Crystals were flash-cooled in liquid nitrogen, and data were collected at 100 K at beamline ID14EH1 of the European Synchrotron Radiation Facility (ESRF; Grenoble, France) and at beamline X10SA of the Swiss Light Source (SLS; Villigen, Switzerland). For phasing, anomalous data of crystal form 1 were collected at wavelengths corresponding to peak (λ = 0.9789 Å), inflection (λ = 0.9796 Å), and high-energy remote (λ = 0.9764 Å) of the selenium K-edge. Selenium-labeled crystals diffracted to 2.4 Å resolution at the SLS. All data were indexed, integrated, and scaled with XDS (*23*).

Structure Solution and Refinement. The structure was solved from anomalous data (Supporting Information Table S1) using XPREP (Bruker Analytical X-ray Solutions), SHELXD (*24*), and SHARP (*25*). An initial model was built manually by remodeling a polyalanine version of PDB entry 1SML (*26*) shifted into the initial electron density, followed by alternating rounds of refinement in REFMAC5 (*27*) and manual correction in O (*28*) and COOT (*29*). The structure was refined to R_{work} = 12.0% and R_{free} = 16.9%; the complex of the E182A mutant with bis-pNPP was refined to R_{work} = 15.6% and R_{free} = 19.6%. Crystal form 2 was phased by molecular replacement with PHASER (*30*) using the protein model of crystal form 1. The structure was refined to R_{work} = 15.1% and R_{free} = 21.1%. Data collection and refinement statistics are summarized in Table 1 and Supporting Information Table S1.

Identification of Iron Atoms in the Active Center of PqsE. The identity of two octahedrally coordinated metal atoms in the active center of recombinant PqsE was determined by inductively coupled plasma mass spectrometry (ICP-MS) on an Element2 instrument from Thermo Electron Corp. equipped with a pneumatic nebulizer (Micromist; Cetac, Omaha, NE) operated at a sample flow rate of 200 μL/min. This confirmed the presence of only Fe (Fe, Mg, Ca, Mn, Ni, Cu, Zn examined). Second, crystals of PqsE were analyzed by X-ray fluorescence scanning on beamline X10SA of the SLS. Strong fluorescence was only observed at the K-edge of iron (Supporting Information Figure S1). In addition, the anomalous electron density around

Table 1: Data Collection and Refinement Statistics[a]

	WT, crystal form 1	E182A/bis-pNPP complex	WT, crystal form 2
Data Collection[b]			
space group	$P3_221$	$P3_221$	$P2_1$
cell dimensions			
a, b, c (Å)	61.10, 61.10, 145.70	60.98, 60.98, 146.82	44.76, 66.09, 110.26
α, β, γ (deg)	90, 90, 120	90, 90, 120	90, 97.19, 90
resolution (Å)	20−1.57 (1.67−1.57)	20−1.8 (1.9−1.8)	20−2.1 (2.2−2.1)
R_{merge}	5.1 (29.0)	5.3 (37.7)	11.3 (39.5)
$I/\sigma I$	24.1 (6.2)	25.7 (4.3)	13.7 (4.6)
completeness (%)	98.8 (93.3)	99.9 (99.9)	97.8 (97.5)
redundancy	8.5 (6.0)	10.8 (6.8)	3.0 (3.0)
Refinement			
resolution (Å)	20−1.57	20−1.8	20−2.1
no. of reflections	42142	28614	34787
R_{work}/R_{free}	12.0/16.9	15.6/19.6	15.1/21.1
no. of atoms			
protein	2458	2411	4855
ligand/ion	11	25	22
water	346	224	376
B-factors			
protein	22	32	31
ligand/ion	17	44	28
water	40	40	42
rms deviations			
bond lengths (Å)	0.027	0.027	0.019
bond angles (deg)	2.089	1.931	1.731
PDB access code	2Q0I	3DH8	2Q0J

[a]WT: wild-type protein. For multiple wavelength anomalous data collection statistics, refer to the Supporting Information (Table S1). [b]All data sets were collected from single crystals. Values in parentheses refer to the highest resolution shell.

the two metal ions was compared and found to be equal for both atoms in data sets of crystal form 1 collected at the K-edges of iron, zinc, and selenium and at 0.934 Å (fixed wavelength at ID14EH1 of the ESRF). Finally, 2 equiv of iron was also discovered by EPR (Supporting Information Figure S2) and with 1,10-phenanthroline (Supporting Information Figure S3) as outlined in the next paragraph.

Determination of the Iron Oxidation State. The oxidation state of the two iron atoms bound to PqsE was probed with two different methods. First, recombinant PqsE was analyzed by electron paramagnetic resonance spectroscopy (EPR). Recombinant protein (approximately 300 μM) was transferred into 2 mm EPR Suprasil quartz tubes, degassed by several freeze−pump−thaw cycles on a vacuum line, and sealed under vacuum. X-band (9−10 GHz) continuous wave EPR spectra were recorded on a Bruker Biospin Elexsys E680 EPR spectrometer fitted with a 3 mm split-ring (ER4118X-MS-3-W1) resonator (Supporting Information Figure S2). Calibration of the magnetic field and the microwave frequency were achieved by a Bruker ER035 M teslameter and a Bruker microwave frequency counter, respectively. Low-temperature measurements were performed in an Oxford CF-935 helium gas-flow cryostat. The temperature was regulated to ±0.1 K by an Oxford Instruments ITC-503 temperature controller. Calibration of the magnetic field for precise *g*-value determination was performed with a Li:LiF standard.

The oxidation state of the two iron atoms was also investigated with 1,10-phenanthroline, which forms a colored Fe(II) complex that can be quantified at 512 nm (*31*). The assay was calibrated with $Fe(II)(NH_4)_2(SO_4)_2$ (Mohr's salt). WT- or E182A-PqsE (38 μM) in 50 mM Tricine, pH 8.5, was incubated with 1 mM 1,10-phenanthronline from a 100 mM stock in DMSO in the presence or absence of 6 M urea to release iron by unfolding and/or 2 mM $Na_2S_2O_4$ to reduce Fe(III) to Fe(II), and the absorption at 512 nm was monitored in a UV/vis spectrophotometer for 20−60 min (Supporting Information Figure S3A,B).

Isothermal Titration Calorimetry (*ITC*). ITC was employed to detect ligands with dissociation constants $K_D \leq 100$ μM. Measurements were performed at 25 °C in a VP-ITC system from MicroCal LLC. Potential ligands were diluted to 1 mM concentration in gel filtration buffer with addition of either DMSO or PEG 400 where necessary and then titrated to PqsE diluted to 100 μM in the same buffer. All solutions were degassed prior to loading into the apparatus. The system was allowed to equilibrate for at least 30 min, and measurements were started with an initial 2 μL injection, followed by injections of 8 μL at 4 min intervals. An example titration with anthranilic acid is shown in Supporting Information Figure S4. Because a benzoate-shaped ligand was found in the crystal structure but benzoate showed no binding under these conditions, the titration with benzoic acid was repeated using doubled concentration of protein and ligand in 100 mM Tris-HCl, pH 7.5.

Binding and Turnover Tests with Potential Substrates of PqsE. Various substances from the context of quorum sensing in *P. aeruginosa* and molecules containing a benzoate moiety were tested for binding and turnover with PqsE. Analysis involved ITC as described above, HPLC on a Waters system equipped with a ProntoSIL 120-5-C18-Aq 5 μm column (Bischoff Analysentechnik), or HPLC-coupled ESI mass spectrometry (Agilent 1100 HPLC system, FINNIGAN LCQ Advantage MAX mass spectrometer, Macherey-Nagel Nucleodur C18 gravity 3 μm 125/4 column). One millimolar compound was incubated with 40 μM PqsE, and samples were injected in 1 h intervals for 3 h and also after overnight incubation. Turnover was judged by comparing peak areas of substrates and potential products from the UV/vis detector and ion currents of the parent m/z value. This method is expected to detect 10% of substrate turnover or less, corresponding to $k_{cat} \geq 0.014$ min^{-1}. Controls included incubation of the compound in the absence of enzyme. PQS and cyclic-di-GMP were kind gifts of F. Bredenbruch and M. Mohr; other chemicals were purchased from Sigma, Alfa Aesar, Serva, Acros, and Frontier Scientific. Results are summarized in Supporting Information Tables S2 and S4−6.

Screen for Hydrolytic Activity of PqsE. The activity of PqsE against a set of general chromogenic substrates was tested to assess PqsE's hydrolytic capacity. This method aims at identifying phosphatases, phosphodiesterases, proteases, and esterases (*32*). In addition, nitrocefin was included to test PqsE for β-lactamase activity (Supporting Information Table S3). PqsE was applied at 40 μM concentration, and assays were performed at 25 °C to avoid precipitation of the protein. The screens were allowed to react for several hours and then inspected by eye or in a spectrophotometer.

Analysis of Phosphodiesterase Activity. Optimum conditions for bis(*p*-nitrophenyl) phosphate (bis-pNPP) hydrolysis were determined by varying pH and metal composition. As a result of these initial experiments, subsequent tests were performed in 50 mM Tricine, pH 8.5, and 2 mM $MnCl_2$. Enzyme

parameters for bis-pNPP hydrolysis were determined by varying the substrate concentration and following the absorption of *p*-nitrophenolate at 405 nm (ε_{405} = 18500 M^{-1} cm^{-1}; Table 2).

Other potential phosphodiesterase substrates were tested by following the reaction with HPLC and HPLC-MS as described above or by agarose gel electrophoresis where appropriate. Negative controls of DNA degradation included incubation with reaction buffer, reaction buffer supplemented with 0.5 mM $FeSO_4$ but excluding PqsE to exclude DNA degradation due to Fenton chemistry, and reactions including PqsE and EDTA or ATP to inhibit the enzyme (Supporting Information Figures S4 and S5 and Table S4).

Analysis of Thioesterase Activity. Thioesterase activity was measured in 50 mM Tricine, pH 8.5, and 2 mM $MnCl_2$ by reacting emerging free thiols with excess 5,5′-dithiobis(2-nitrobenzoic acid) (DTNB, Ellman's reagent) and following the release of 2-nitro-5-thiobenzoate at 412 nm (ε_{412} = 14150 M^{-1} cm^{-1}). Substrates were employed to a maximum concentration of 1 mM, PqsE was added to 0.2 or 2 μM, and the concentration of DTNB was 2 mM. Incubation without substrate served as control to determine background degradation of DTNB. Results of these experiments are summarized in Supporting Information Tables S5 and S6.

Metal Reconstitution Studies. Reconstitution experiments were performed with the E182A mutant of PqsE, using the bis-pNPP-based phosphodiesterase test for monitoring activity since this provided the most robust assay. Three different methods were employed to produce reconstituted enzyme. First, iron-free apoenzyme was prepared by incubation of 100 μM protein with 2 mM $Na_2S_2O_4$ and 1 mM 1,10-phenanthroline, followed by removal of excess reagents with a NAP5 gel filtration column in 50 mM Tricine, pH 8.5. The protein was then incubated with various 1 mM salts ($CoCl_2$, $CaCl_2$, $MgCl_2$, $CuSO_4$, $CdCl_2$, ZnSO4, $MnCl_2$, $Fe(II)(NH_4)_2(SO_4)_2$, $Fe(III)(NH_4)_3(SO_4)_3$), either applied alone or in combination.

Second, 1−5 μM protein in 50 mM Tricine, pH 8.5, was carefully titrated with EDTA until the phosphodiesterase activity was significantly reduced. The required EDTA concentration was 50 μM. For reactivation, the deactivated protein was incubated with 1 mM metal ions listed above, and phosphodiesterase activity was reassessed.

Third, 1−5 μM protein in 50 mM Tricine, pH 8.5, was incubated with increasing concentrations of $CoCl_2$, $MnCl_2$, or $Fe(II)(NH_4)_2(SO_4)_2$, and phosphodiesterase activity at saturating bis-pNPP concentration (1 mM) was measured to derive concentration-dependent activation profiles. In order to determine the residual iron concentration of the Co^{2+}-activated enzyme, 100 μM protein was first incubated with 10 mM $CoCl_2$ on ice for 30 min and then passed through a NAP5 column. The iron content was quantified with 1,10-phenanthroline as described above. In addition, phosphodiesterase activity with and without reincubation with $CoCl_2$ was determined to investigate whether Co^{2+} bound in the initial activation experiment is lost in the reagent removal step.

Analysis of PqsE Mutants in P. aeruginosa PAO1. The effect of active site mutations on the regulatory activity of PqsE was assessed by quantification of pyocyanin in a Δ*pqsE* transposon mutant of *P. aeruginosa* PAO1 (*33*) transformed with pUC-*pqsE* plasmids containing the desired mutations. Five milliliters of LB media supplemented with 100 μg/mL ampicillin in a 25 mL Erlenmeyer flask was inoculated to OD_{660} = 0.05 with overnight culture and incubated for 18 h at 37 °C under vigorous shaking (170 rpm), resulting in similar cell density of all strains investigated. Cells were separated by centrifugation, and 500 μL of culture supernatant was extracted with 300 μL of chloroform. The organic phase was acidified with 100 μL of 0.2 M HCl, and pyocyanin was quantified at 520 nm as previously described (*19*). All mutants were also produced as recombinant proteins in *E. coli* to ensure that loss of activity was not due to improper folding.

Table 2: Kinetic Parameters of PqsE Variants with Bis-pNPP[a]

protein	K_M (μM)	k_{cat} (min^{-1})
PqsE (Ni-NTA purification)	124	0.011
MBP-PqsE (with tag)	346	0.009
MBP-PqsE (tag removed)	405	0.011
GST-PqsE	156	0.011
STREPII-tag-PqsE	507	0.011
PqsE-E182A	208	12.4

[a]Data were measured in 50 mM Tricine, pH 8.5, at room temperature and in the presence of 2 mM $MnCl_2$.

RESULTS

Overall Structure of PqsE. PqsE was crystallized in two different colorless crystal forms, and the structure was refined to 1.6 Å resolution (Table 1). As predicted previously (*21*), the overall fold resembles that of a typical metallo-β-lactamase hallmarked by an $\alpha\beta/\alpha\beta$ sandwich core structure, indicating that PqsE exerts its regulatory effect through an unidentified enzymatic activity. In comparison to other members of the metallo-β-lactamase superfamily, the monomeric PqsE possesses two additional α-helices at its C-terminus that cover the active center. These two helices limit accessibility to the active site and might be able to move as a lid that opens and closes for substrate binding. In the presumably closed form observed here, two tunnels of approximately 10 and 18 Å length approach the active center from opposite sides of the protein, suggesting that the natural substrate of PqsE is an extended molecule (Figure 2A). Interestingly, in some of the data sets collected for this study the wider and longer of these two tunnels binds a copurified ligand, which was assigned as benzoate from the shape of its electron density (Figure 2B). Its location coincides with the substrate binding site in related enzymes, and its carboxylate group participates in coordinating one of the two metal ions of the active center. The ligand was observed in both crystal forms, and its occupancy seemed to be correlated to the age of the protein batch and the type of media used for production of the recombinant PqsE. While it reaches approximately 70% in crystals from protein freshly prepared from TB, no ligand was present in seleno-L-methionine-labeled PqsE produced in LeMaster media.

Recombinant PqsE Binds Two Iron Atoms in Its Active Center. Both of the metal ions contained in the active center of PqsE are octahedrally coordinated. They were identified as iron by inductively coupled plasma mass spectrometry (ICP-MS), anomalous diffraction data, X-ray fluorescence, and electron paramagnetic resonance (EPR) spectroscopy and through photometric detection with 1,10-phenanthroline (Supporting Information Figures S1−3). Other metals could not be detected. The sample submitted to ICP-MS revealed only substoichiometric amounts of iron, which indicates that its binding to PqsE is relatively weak. This is also reflected in the observation that only freshly prepared protein could be crystallized and crystals decayed quickly.

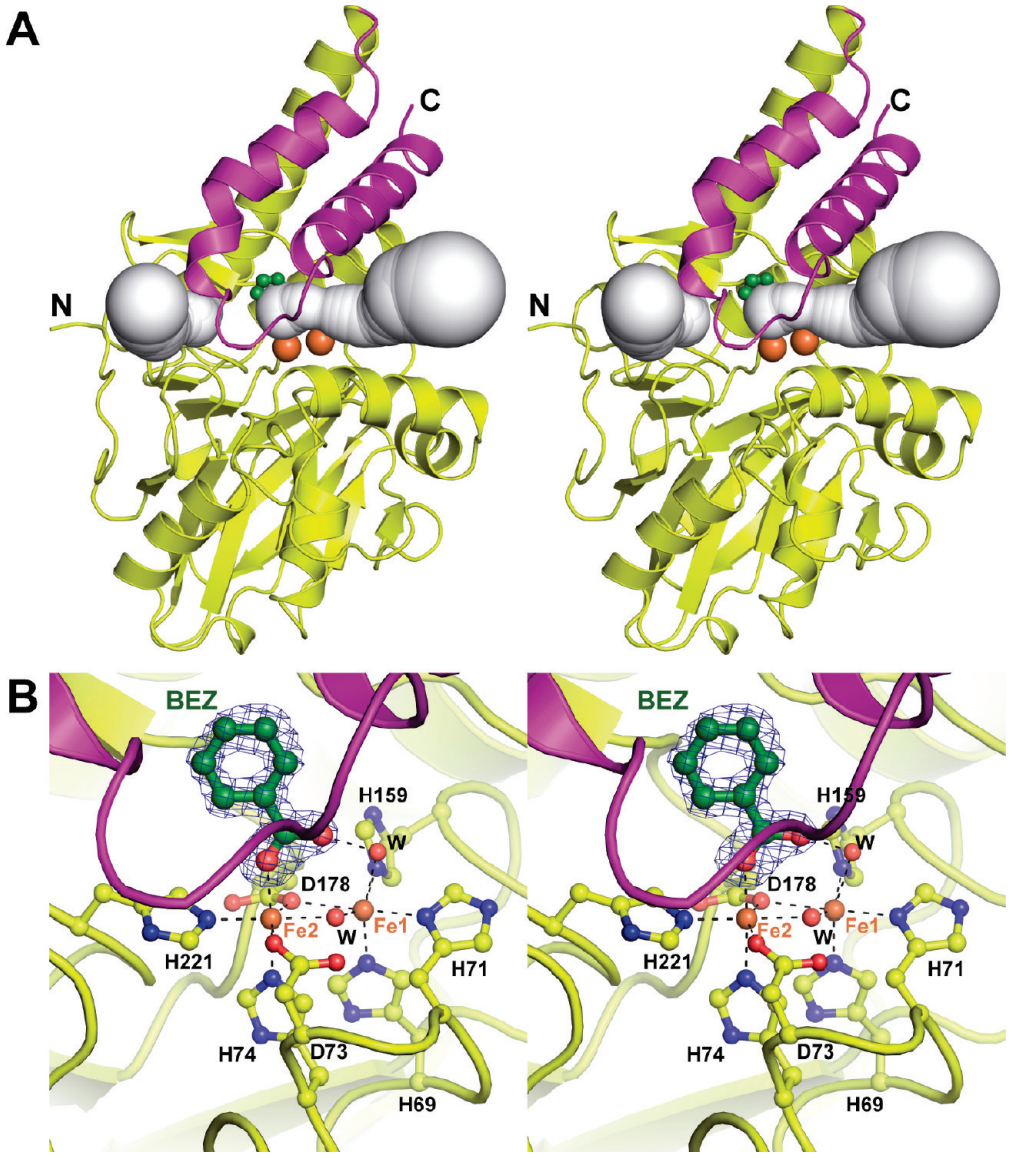

FIGURE 2: Crystal structure of PqsE. (A) Stereo diagram of the overall structure. The two C-terminal helices shown in magenta could act as a lid that controls access to the active site. Gray: two tunnels approaching the active center. (B) Stereo diagram of the iron binding site in PqsE and $|F_o - F_c|$ electron density of the copurified benzoate-shaped ligand (BEZ). This figure was prepared with PyMOL (*56*) and CAVER (*57*).

In order to determine the oxidation state of the two iron atoms, low-temperature continuous wave EPR spectra were recorded at X-band microwave frequencies. At 10 K, the enzyme gave an EPR signal (signal amplitude $d\chi''/dB_0$ as a function of the magnetic field B_0) centered around 350 mT (Supporting Information Figure S2). The signal is of rhombic symmetry with a sharp peak at 336 mT, a zero-crossing at 351 mT, and a broader minimum centered at 384 mT. The *g*-values extracted from magnetic field calibrated data are 1.93, 1.86, and 1.69 (g_{iso} = 1.83), which is characteristic of an $S = {}^1/_2$ ground-state spin system of an antiferromagnetically coupled mixed-valent Fe(II)Fe(III) center as has been found and discussed in detail for the related mitochondrial glyoxylase II from *Arabidopsis thaliana* (*g*-values 1.93, 1.87, 1.73; PDB entry 1XM8) (*34*). Similar diiron centers are also contained in several otherwise unrelated proteins, e.g., myo-inositol oxygenase (*35*), methane monooxygenase (*36*, *37*), and ubiquinol oxidase (*38*).

The oxidation states were also confirmed with 1,10-phenanthroline, which produces a colored complex with Fe(II) but not with Fe(III): 2 equiv of iron was measured when PqsE was reductively denatured with excess $Na_2S_2O_4$, whereas only 1 equiv was found after nonreductive unfolding with 6 M urea. Here, the second equivalent was detected after reducing the urea-denatured protein with $Na_2S_2O_4$ (Supporting Information Figure S3A,B).

The two iron atoms bound to the active center are 3.5 Å away from each other, bridged by a water molecule and by the side chain of D178. The remaining residues through which PqsE coordinates the iron atoms consist of a conserved sequence motif ^{69}HXHXDH^{74}~H^{159}~H^{221} (*39*), of which H69, H71, and H159 plus an additional water coordinate Fe1, while Fe2 is coordinated by D73, H74, and H221 (Figure 2B). This binding motif is most typical for proteins containing two zinc ions (Supporting Information Table S7) (*39*); however, since the assignment of the Fe(II)Fe(III) center in recombinant PqsE was unambiguous and the number of functionally assigned proteins with two-iron centers within the superfamily is relatively small, the iron content may hint toward the molecular function of PqsE. Accordingly, functionally related proteins would potentially include rubredoxin:oxygen oxidoreductase ROO from *Desulfovibrio gigas* (*40*), the FprA enzymes from *Moorella thermoacetica* (*41*) and

Methanothermobacter marburgensis (*42*), and also certain structurally more distantly related binuclear metallohydrolases like pig allantoic fluid purple acid phosphatase PPAP (*43*) or the phosphorylcholine esterase domain of choline binding protein E from *Streptococcus pneumoniae* Pce (*44*). ROO and FprA belong to the family of flavodiiron proteins, a class of enzymes involved in the detoxification of NO and O_2 in bacteria that normally live in anaerobic environments. They contain a second, flavin-binding domain that participates in the redox reactions that these enzymes catalyze (*45*). Since this domain is absent in PqsE and the regulatory effect of PqsE is not restricted to anaerobic conditions, it is unlikely that PqsE is an oxidoreductase but belongs to the large hydrolase group within the metallo-β-lactamase family instead.

Search for Enzymatic Activity. In order to determine which chemical reaction PqsE catalyzes, we first assayed a selection of compounds including, among others, PQS and homoserine lactones for binding and turnover (Supporting Information Table S2). PQS was recently shown to bind and activate the transcription factor PqsR (MvfR) (*14*) but was nevertheless chosen because the binding site of PqsE seems perfectly suited for a PQS-shaped molecule. Homoserine lactones were tested because quorum quenching metallo-β-lactamase family members that hydrolyze homoserine lactones have been described in the literature (*46*−*48*), and a link between C4-AHL/RhlR and PqsE signaling has recently been established (*19*).

Of the molecules tested for binding to PqsE, only anthranilate (K_D = 10.7 ± 1.1 μM; Supporting Information Figure S4) and benzoate (K_D = 29.1 ± 4.8 μM) showed relatively weak binding (Supporting Information Table S5). The reason for the fact that the copurified benzoate-shaped ligand could nevertheless be observed in the crystal structure is unclear at present. It is possible that the assignment as benzoate is not correct, which cannot be assessed from the available electron density.

We next extended our search for substrates of PqsE by employing a set of general chromogenic substrates for a broader assessment of hydrolytic capacity (*32*). In this screen, PqsE displayed low activity against bis(*p*-nitrophenyl) phosphate (bis-pNPP), indicative of phosphodiesterase activity (Figure 3B, Table 2, and Supporting Information Table S3). The activity was highest at basic pH and when Mn^{2+} was included in the buffer, even if other experiments clearly showed that manganese was not bound to the purified protein. Additional experiments addressing this observation are described below.

Because the activity toward bis-pNPP was very low (K_M = 124 μM, k_{cat} = 0.011 min^{-1}; addition of 2 mM $MnCl_2$), several controls were performed to exclude that it was due to a copurified impurity. First, hydrolysis of bis-pNPP was also observed with protein from dissolved PqsE crystals. Second, PqsE was fused C-terminally to glutathione *S*-transferase, maltose-binding protein, or the Strep-tag II peptide for orthogonal affinity purification. The purified fusion proteins retained phosphodiesterase activity at a level comparable to that of the wild-type protein (Table 2). Third, we generated several mutants of PqsE of which one, E182A, had considerably higher activity toward bis-pNPP than the wild-type protein (K_M = 208 μM, k_{cat} = 12.4 min^{-1}). It was also possible to determine the crystal structure of this mutant in complex with bis-pNPP, which demonstrates that removal of the glutamate side chain increases the space available for substrate binding, explaining the elevated activity. The phosphate group of bis-pNPP coordinates both iron atoms such that the bridging water molecule is positioned for an SN_2 reaction at the phosphorus atom. However, potential catalytic residues that could participate in the chemistry of the hydrolysis reaction like in many related enzymes cannot be identified in the immediate vicinity of the metal center (Figure 3A, Supporting Information Figure S8).

Activity toward Cellular Phosphodiesters. We tried to narrow PqsE's specificity against phosphodiesters down further by testing the hydrolysis of several phosphodiesters occurring in the cell. Of the compounds investigated (Supporting Information Table S4), only single- and double-stranded DNA together with RNA were cleaved by PqsE, albeit slowly (Figure 3C, Supporting Information Figure S5), which is not surprising since the substrate binding tunnel seems too narrow to admit access of double-stranded oligonucleotides. This may explain why the turnover pattern observed with DNA corresponds to stepwise shortening of the substrate, which could indicate that disruption of base pairing is required and that degradation can only proceed from strand ends. Addition of EDTA or ATP inhibited PqsE (Supporting Information Figure S6).

Activity toward Benzoate Derivatives. In order to explore the significance of the copurified benzoate-shaped ligand found in the crystal structure, PqsE was incubated with a number of benzoate derivatives including, among others, esters, amides, and thioesters, and turnover was probed by HPLC or HPLC-MS (Supporting Information Table S5). Of the molecules tested, significant hydrolysis was only observed with *S*-(4-nitrobenzoyl)mercaptoethane (S-(4NB)-ME); K_M = 14 μM, k_{cat} = 7.2 min^{-1}; addition of 2 mM $MnCl_2$). While the presence of Mn^{2+} led to higher reaction rates similar to what was found for phosphodiesterase activity, k_{cat} was considerably lower in the E182A mutant (K_M = 13 μM, k_{cat} = 0.18 min^{-1}).

Activity toward Cellular Thioesters. Thioester intermediates play an important role in numerous anabolic and catabolic pathways, e.g., in fatty acid degradation and synthesis, the citric acid cycle, nonribosomal peptide, and polyketide biosynthesis. Since these intermediates mostly occur as phosphopantetheine derivatives and the phosphopantetheine moiety seems well suited to bind the longer of the two active site tunnels, a number of commercially available acyl-coenzyme A representatives were incubated with PqsE (acetyl-CoA, malonyl-CoA, benzoyl-CoA), but PqsE did not hydrolyze any of these compounds (Supporting Information Table S6).

Thioesterase activity is well established for Zn^{2+}-dependent metallo-β-lactamases of the glyoxalase II type (*39*). These enzymes are involved in the detoxification of α-ketoaldehydes like methylglyoxal, where they hydrolyze the glutahione adduct L-lactoylglutathione. PqsE was, however, also not active against this compound.

Metal Reconstitution Studies. The observation that exogenously supplied Mn^{2+} significantly increased PqsE's hydrolytic activity despite identifying two iron atoms bound to the active center prompted additional experiments studying the metal preference of PqsE. Such experiments may provide an indication that the Fe(II)/Fe(III) center is an artifact of heterologous protein expression as has been reported for other recombinant metalloenzymes (*49*). Hydrolysis of bis-pNPP by E182A-PqsE was used to monitor reconstitution because this gave the most reliable activity assay. However, since the true substrate of PqsE is not known, the following results are of preliminary nature and should be interpreted with care.

The enzyme was first made iron-free by reductively removing bound iron with $Na_2S_2O_4$ and 1,10-phenanthroline. Reconstitution

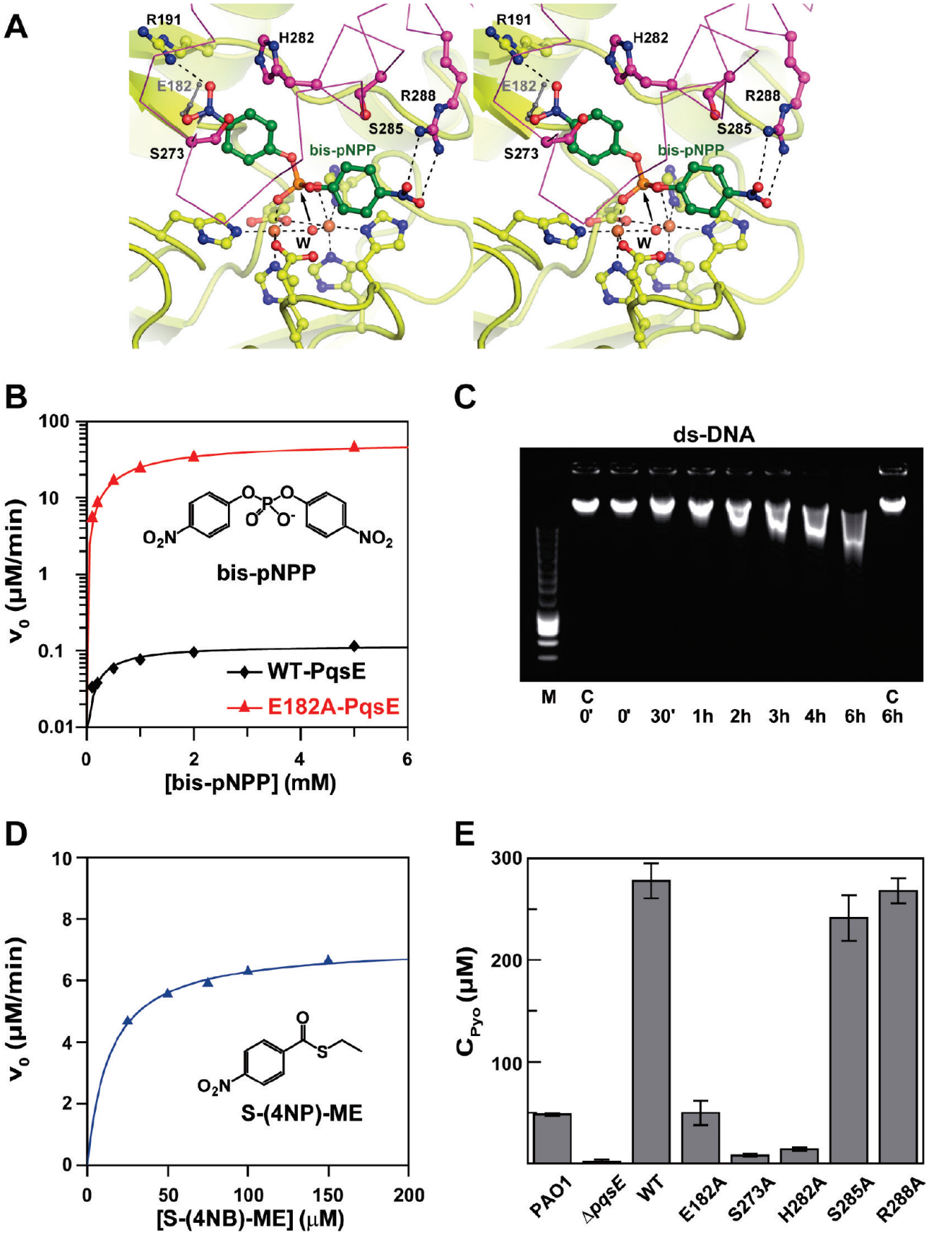

FIGURE 3: Hydrolytic activity of PqsE. (A) Stereo diagram of bis-pNPP bound to the active center of the E182A mutant of PqsE. E182 from the wild-type structure is shown in gray. Polar residues lining the substrate binding site are indicated. (B) Michaelis−Menten plot of bis-pNPP hydrolysis by PqsE and its E182A mutant. Note the logarithmic scale of the ordinate. (C) Hydrolysis of ds-DNA by PqsE. 3.5 μg of λ-phage DNA was incubated with 50 μM PqsE, and samples were removed after the times indicated. Key: C, control (buffer); M, marker. (D) Michaelis−Menten plot of S-(4NP)-ME hydrolysis. (E) Pyocyanin production of *P. aeruginosa* PAO1 and a Δ*pqsE* transposon mutant of *P. aeruginosa* PAO1 and the same mutant transformed with pUC plasmids containing wild-type *pqsE* (WT) or *pqsE* mutated at the indicated positions.

Table 3: Reconstitution of E182A-PqsE with Divalent Cations[a]

E182A-PqsE reconstituted with	relative k_{cat}/K_M (*x*-fold)
–	1
Fe^{2+}	3.3
Mn^{2+}	7.9
Ni^{2+}	1.9
Co^{2+}	9.7

[a]The protein was deactivated with EDTA, and phosphodiesterase activity against bis-pNPP was measured after reconstitution with the indicated cations.

by incubation with Fe(III)-containing combinations of metal salts restored only low levels of activity, suggesting that more sophisticated protocols will be required to refold apo-PqsE. We therefore employed a more careful method of deactivating the enzyme, titrating E182A-PqsE with EDTA until phosphodiesterase activity was abolished. Reconstitution with transition metals showed that activity can be recovered and that incubation with Co^{2+} was even more effective than Mn^{2+}, rendering E182A-PqsE approximately 3-fold more active than Fe^{2+} or Ni^{2+}, which restored activity to comparable levels as judged by k_{cat}/K_M values (Table 3). While this explains the observation that Mn^{2+} increased phosphodiesterase activity in the earlier assays, it is worth noting that reconstitution with Fe^{2+} from $Fe(II)(NH_4)_2(SO_4)_2$ also lead to significantly higher activity than was measured before deactivation of the protein with EDTA. This suggested that the protein had lost iron in the course of purification, and indeed, reassessment of the iron content of the nondeactivated protein with 1,10-phenanthroline/$Na_2S_2O_4$ detected less than 60% of the expected value, with the Fe(II)/Fe(III) ratio being approximately 1:3 (Supporting Information Figure S3B).

Reconstitution with Zn^{2+}, which is the most common metal in closer relatives of PqsE (Supporting Information Table S7), was not successful because the apoprotein had to be kept at basic pH to avoid precipitation.

Half-maximal phosphodiesterase activity was reached with approximately 280 μM Co^{2+} (Supporting Information Figure S3C), and when the protein was treated with a large excess of Co^{2+}, the Fe(III) content was not altered whereas approximately half of the initial Fe(II) was lost (Supporting Information Figure S3B). Removal of excess Co^{2+} lead to loss of activity, which could be reversed by adding fresh $CoCl_2$.

Effect of Mutations on the Regulatory Activity of PqsE. Because the activity toward all tested substrates is rather low, the assessment of active site mutations using these compounds may be misleading with respect to the regulatory effect of PqsE. We therefore probed these mutants indirectly by quantifying the PqsE-controlled virulence factor pyocyanin in a Δ*pqsE* transposon mutant of *P. aeruginosa* PAO1 to which *pqsE* had been reintroduced from a pUC plasmid (Figure 3C). Constitutive expression of *pqsE* led to significantly higher amounts of pyocyanin with respect to the parental *P. aeruginosa* PAO1 strain. Next, we tested the importance of polar residues in the vicinity of the substrate binding site since these amino acids could participate in catalysis by protonating a negatively charged hydrolysis intermediate or by binding and positioning PqsE's substrate. Mutagenesis revealed that S273 and H282 play an important role while S285 and R288 are not required. Interestingly, similar to the decrease in thioesterase activity described above, the amount of pyocyanin formed by the E182A mutant was reduced to approximately 15% of the wild-type protein, while this variant was 1000-fold more efficient in hydrolyzing bis-pNPP (see above).

DISCUSSION

While our attempts to identify the natural substrate of PqsE were unsuccessful, the data presented here still provide valuable new insight into this important regulatory protein. First, the overall structure of PqsE is unusual because the two additional helices at its C-terminus render its active center relatively buried in comparison to other metallo-β-lactamase proteins (Supporting Information Figure S7). This suggests that desolvation makes an important contribution to substrate activation in PqsE, and indeed no water molecules other than those coordinating the metal ions are found in the immediate vicinity of the active center.

Barring knowledge about the native function, it is not possible to assign the natural metal composition of PqsE's binuclear reaction center from the reconstitution experiments described above. It is, however, interesting that recombinant PqsE contained a redox-stable Fe(II)/Fe(III) center, whereas other proteins with the same first metal coordination sphere usually depend on zinc (Supporting Information Table S7 and Figure S8). Clearly, not only the immediate metal binding residues determine the composition of the active center in this protein family.

With the data presented here, it is not fully possible to rule out that PqsE requires a third cation for activity. However, such a scenario seems unlikely since only one other related enzyme with an adventitiously bound third cation from the crystallization buffer has been reported to date (PDB entry 1QHW) (*50*). Therefore, the finding that several transition metals restored activity to comparable levels likely is a property that PqsE shares with other binuclear metallohydrolases that were found to possess a tightly bound Fe(III) and an exchangeable divalent cation in their binuclear center (*51*). This is also indicated by the observation that incubation with excess Co^{2+} replaced a large fraction of Fe(II) whereas the Fe(III) content was unchanged (Supporting Information Figure S3B). Taken together, this suggests that the native composition of the reactive center in PqsE and related enzymes is determined by metal availability within the cell.

Next, the observation of a copurified benzoate-shaped ligand in the active center is interesting because it could indicate that the regulatory effect of PqsE is mediated through a chorismate-derived molecule. In microorganisms and plants, chorismate is a central metabolite that is distributed into numerous tightly regulated pathways (*52*), and several of its derivatives have regulatory roles either as activators of specific transcription factors in a manner similar to PQS or by acting as allosteric feedback inhibitors, e.g., the aromatic amino acids, which inhibit the first step of chorismate biosynthesis in the shikimate pathway (*53*). The fact that many of the pathways that utilize chorismate are conserved across different microorganisms could explain why Farrow et al. observed PqsE-dependent coactivation of a RhlR/rhlA′-lacZ reporter system in the heterologous host *E. coli*, which does not possess a *pqs* operon itself (*19*).

Further, our results provide evidence that PqsE exerts its physiological role by acting as a hydrolase. We observed phosphodiesterase activity toward DNA and RNA, but this activity seems too low to be meaningful, even if metallo-β-lactamases that play physiological roles in DNA or RNA processing are

known (*54*), and many other binuclear metallohydrolases have been assigned as phosphoesterases (*43*, *44*). More promising seems the finding of slightly higher levels of thioesterase activity toward a para-substituted benzoate derivative, which in the light of the copurified benzoate-shaped ligand and the mutagenesis data shown in Figure 3C suggests that S273, H282, and possibly also E182 are required to bind and position a meta- or para-substituted benzoate derivative for hydrolysis of a thioester linkage. Thioesters play important roles in countless degradative and biosynthetic pathways, e.g., in fatty acid metabolism or in polyketide and nonribosomal peptide biosynthesis and also in the turnover of phenylalanine to benzoate. In these pathways the carboxylic acid is linked to a phosphopantetheine moiety, which in turn is either bound to a carrier protein or to 3-phospho-AMP in coenzyme A. The phosphopanthetheine group itself is an extended arm of approximately 17 Å length, making it ideally suited to bind to the longer tunnel leading to the active site of PqsE. Even if none of the tested CoA derivatives was hydrolyzed in our experiments, it is therefore tempting to speculate that PqsE functions by interfering with one of these pathways, i.e., by sending a metabolic rather than a transcriptional signal as in other quorum sensing systems. Because many of the possible pathways are conserved, it would not be surprising that PqsE also showed an effect when overexpressed in the *E. coli* RhlR/rhlA′-lacZ reporter system mentioned above (*19*).

Finally, the crystal complex of E182A-PqsE with bis-pNPP provides mechanistic insight into the hydrolytic activity of PqsE. Similar to findings in other metallohydrolases, the bridging water molecule is perfectly positioned for hydrolytic attack of the substrate, and the positive charge of the neighboring metal ions will increase its nucleophilicity. In agreement with mechanistic studies performed with other binuclear metallohydrolases, the emerging negative charge of the transition state in hydrolysis is expected to be stabilized through coordination with the dimetal center (*55*), and it is conceivable that the phosphate moiety of the bis-pNPP complex mimics the corresponding tetrahedral intermediate in thioester hydrolysis. However, unlike many other metallohydrolases, the active center of PqsE lacks a protonating residue in the immediate vicinity of the metal ions. Related enzymes utilize such a residue (generally a histidine, Supporting Information Figure S8) to stabilize the negatively charged leaving group, which may explain why we could only observe activity toward substrates with very good leaving groups such as *p*-nitro-substituted phenolates or benzoates.

We are currently analyzing these findings further to derive and test new hypotheses for the function of PqsE in our laboratories.

ACKNOWLEDGMENT

We thank Roger S. Goody for generous support of this project and Ingrid Hoffmann together with Petra Geue for technical assistance. The help of the X-ray communities at the Max-Planck-Institutes of Molecular Physiology (Dortmund, Germany) and for Medical Research (Heidelberg, Germany) with data collection and Alke Meents and Ehmke Pohl with X-ray fluorescence scans is gratefully acknowledged. We thank the European Synchrotron Radiation Facility (Grenoble, France) and the Swiss Light Source (Villigen, Switzerland) for access to their beamlines. Michael Morr and Florian Bredenbruch are acknowledged for providing PQS and cyclic di-GMP.

SUPPORTING INFORMATION AVAILABLE

Multiple wavelength anomalous diffraction data collection statistics, X-ray fluorescence of PqsE crystals at the iron K-absorption edge, iron content and Co^{2+} activation studies, electron paramagnetic resonance spectra, isothermal titration calorimetry of anthranilate, inhibition of DNase activity by EDTA and ATP, structural comparison with a typical Zn^{2+}-containing metallohydrolase, and results of binding and activity assays. This material is available free of charge via the Internet at http://pubs.acs.org.

REFERENCES

1. Emerson, J., Rosenfeld, M., McNamara, S., Ramsey, B., and Gibson, R. L. (2002) *Pseudomonas aeruginosa* and other predictors of mortality and morbidity in young children with cystic fibrosis. *Pediatr. Pulmonol. 34*, 91–100.
2. van Delden, C. (2004) in *Pseudomonas* (Ramos, J. L., Ed.) pp 3−45, Kluwer Academic/Plenum Publishers, New York.
3. Drenkard, E. (2003) Antimicrobial resistance of *Pseudomonas aeruginosa* biofilms. *Microbes Infect. 5*, 1213–1219.
4. Diggle, S. P., Heeb, S., Dubern, J. F., Fletcher, M. P., Crusz, S. A., Williams, P., and Camara, M. (2008) in *Pseudomonas*. Model Organism, Pathogen, Cell Factory (Rehm, H. A., Ed.) pp 167−194, Wiley-VCH, Weinheim.
5. Girard, G., and Bloemberg, G. V. (2008) Central role of quorum sensing in regulating the production of pathogenicity factors in *Pseudomonas aeruginosa*. *Future Microbiol. 3*, 97–106.
6. Bassler, B. L., and Losick, R. (2006) Bacterially speaking. *Cell 125*, 237–246.
7. Pesci, E. C., Milbank, J. B., Pearson, J. P., McKnight, S., Kende, A. S., Greenberg, E. P., and Iglewski, B. H. (1999) Quinolone signaling in the cell-to-cell communication system of *Pseudomonas aeruginosa*. *Proc. Natl. Acad. Sci. U.S.A. 96*, 11229–11234.
8. Calfee, M. W., Coleman, J. P., and Pesci, E. C. (2001) Interference with *Pseudomonas* quinolone signal synthesis inhibits virulence factor expression by *Pseudomonas aeruginosa*. *Proc. Natl. Acad. Sci. U.S.A. 98*, 11633–11637.
9. McKnight, S. L., Iglewski, B. H., and Pesci, E. C. (2000) The *Pseudomonas* quinolone signal regulates *rhl* quorum sensing in *Pseudomonas aeruginosa*. *J. Bacteriol. 182*, 2702–2708.
10. Gallagher, L. A., McKnight, S. L., Kuznetsova, M. S., Pesci, E. C., and Manoil, C. (2002) Functions required for extracellular quinolone signaling by *Pseudomonas aeruginosa*. *J. Bacteriol. 184*, 6472–6480.
11. Bredenbruch, F., Nimtz, M., Wray, V., Morr, M., Muller, R., and Haussler, S. (2005) Biosynthetic pathway of *Pseudomonas aeruginosa* 4-hydroxy-2-alkylquinolines. *J. Bacteriol. 187*, 3630–3635.
12. Farrow, J. M.III, and Pesci, E. C. (2007) Two distinct pathways supply anthranilate as a precursor of the *Pseudomonas* quinolone signal. *J. Bacteriol. 189*, 3425–3433.
13. Coleman, J. P., Hudson, L. L., McKnight, S. L., Farrow, J. M.III, Calfee, M. W., Lindsey, C. A., and Pesci, E. C. (2008) *Pseudomonas aeruginosa* PqsA is an anthranilate-coenzyme A ligase. *J. Bacteriol. 190*, 1247–1255.
14. Xiao, G., Deziel, E., He, J., Lepine, F., Lesic, B., Castonguay, M. H., Milot, S., Tampakaki, A. P., Stachel, S. E., and Rahme, L. G. (2006) MvfR, a key *Pseudomonas aeruginosa* pathogenicity LTTR-class regulatory protein, has dual ligands. *Mol. Microbiol. 62*, 1689–1699.
15. Cao, H., Krishnan, G., Goumnerov, B., Tsongalis, J., Tompkins, R., and Rahme, L. G. (2001) A quorum sensing-associated virulence gene of *Pseudomonas aeruginosa* encodes a LysR-like transcription regulator with a unique self-regulatory mechanism. *Proc. Natl. Acad. Sci. U.S.A. 98*, 14613–14618.
16. Diggle, S. P., Matthijs, S., Wright, V. J., Fletcher, M. P., Chhabra, S. R., Lamont, I. L., Kong, X., Hider, R. C., Cornelis, P., Camara, M., and Williams, P. (2007) The *Pseudomonas aeruginosa* 4-quinolone signal molecules HHQ and PQS play multifunctional roles in quorum sensing and iron entrapment. *Chem. Biol. 14*, 87–96.
17. Mashburn, L. M., and Whiteley, M. (2005) Membrane vesicles traffic signals and facilitate group activities in a prokaryote. *Nature 437*, 422–425.
18. Mashburn-Warren, L., Howe, J., Garidel, P., Richter, W., Steiniger, F., Roessle, M., Brandenburg, K., and Whiteley, M. (2008) Interaction of quorum signals with outer membrane lipids: insights into prokaryotic membrane vesicle formation. *Mol. Microbiol. 69*, 491–502.

19. Farrow, J. M.III, Sund, Z. M., Ellison, M. L., Wade, D. S., Coleman, J. P., and Pesci, E. C. (2008) PqsE functions independently of PqsR-*Pseudomonas* quinolone signal and enhances the *rhl* quorum-sensing system. *J. Bacteriol. 190*, 7043–7051.
20. Diggle, S. P., Lumjiaktase, P., Dipilato, F., Winzer, K., Kunakorn, M., Barrett, D. A., Chhabra, S. R., Camara, M., and Williams, P. (2006) Functional genetic analysis reveals a 2-alkyl-4-quinolone signaling system in the human pathogen *Burkholderia pseudomallei* and related bacteria. *Chem. Biol. 13*, 701–710.
21. Dubern, J. F., and Diggle, S. P. (2008) Quorum sensing by 2-alkyl-4-quinolones in *Pseudomonas aeruginosa* and other bacterial species. *Mol. Biosyst. 4*, 882–888.
22. Doublie, S. (1997) Preparation of selenomethionyl proteins for phase determination. *Methods Enzymol. 276*, 523–530.
23. Kabsch, W. (1993) Automatic processing of rotation diffraction data from crystals of initially unknown symmetry and cell constants. *J. Appl. Crystallogr. 26*, 795–800.
24. Schneider, T. R., and Sheldrick, G. M. (2002) Substructure solution with SHELXD. *Acta Crystallogr., Sect. D: Biol. Crystallogr. 58*, 1772–1779.
25. de la Fortelle, E., and Bricogne, G. (1997) in Methods in Enzymology, pp 472−494, Academic Press, New York.
26. Ullah, J. H., Walsh, T. R., Taylor, I. A., Emery, D. C., Verma, C. S., Gamblin, S. J., and Spencer, J. (1998) The crystal structure of the L1 metallo-beta-lactamase from *Stenotrophomonas maltophilia* at 1.7 Å resolution. *J. Mol. Biol. 284*, 125–136.
27. Murshudov, G. N., Vagin, A. A., and Dodson, E. J. (1997) Refinement of macromolecular structures by the maximum-likelihood method. *Acta Crystallogr, Sect. D: Biol. Crystallogr. 53*, 240–255.
28. Jones, T. A., Zou, J. Y., Cowan, S. W., and Kjeldgaard (1991) Improved methods for building protein models in electron density maps and the location of errors in these models. *Acta Crystallogr. A 47* (Part 2), 110–119.
29. Emsley, P., and Cowtan, K. (2004) Coot: model-building tools for molecular graphics. *Acta Crystallogr., Sect. D: Biol. Crystallogr. 60*, 2126–2132.
30. McCoy, A. J., Grosse-Kunstleve, R. W., Storoni, L. C., and Read, R. J. (2005) Likelihood-enhanced fast translation functions. *Acta Crystallogr., Sect. D: Biol. Crystallogr. 61*, 458–464.
31. Merkx, M., and Averill, B. A. (1998) Ga^{3+} as a functional substitute for Fe^{3+}: preparation and characterization of the $Ga^{3+}Fe^{2+}$ and $Ga^{3+}Zn^{2+}$ forms of bovine spleen purple acid phosphatase. *Biochemistry 37*, 8490–8497.
32. Kuznetsova, E., Proudfoot, M., Sanders, S. A., Reinking, J., Savchenko, A., Arrowsmith, C. H., Edwards, A. M., and Yakunin, A. F. (2005) Enzyme genomics: Application of general enzymatic screens to discover new enzymes. *FEMS Microbiol. Rev. 29*, 263–279.
33. Jacobs, M. A., Alwood, A., Thaipisuttikul, I., Spencer, D., Haugen, E., Ernst, S., Will, O., Kaul, R., Raymond, C., Levy, R., Chun-Rong, L., Guenthner, D., Bovee, D., Olson, M. V., and Manoil, C. (2003) Comprehensive transposon mutant library of *Pseudomonas aeruginosa*. *Proc. Natl. Acad. Sci. U.S.A. 100*, 14339–14344.
34. Marasinghe, G. P., Sander, I. M., Bennett, B., Periyannan, G., Yang, K. W., Makaroff, C. A., and Crowder, M. W. (2005) Structural studies on a mitochondrial glyoxalase II. *J. Biol. Chem. 280*, 40668–40675.
35. Thorsell, A. G., Persson, C., Voevodskaya, N., Busam, R. D., Hammarstrom, M., Graslund, S., Graslund, A., and Hallberg, B. M. (2008) Structural and biophysical characterization of human myo-inositol oxygenase. *J. Biol. Chem. 283*, 15209–15216.
36. Dewitt, J. G., Bentsen, J. G., Rosenzweig, A. C., Hedman, B., Green, J., Pilkington, S., Papaefthymiou, G. C., Dalton, H., Hodgson, K. O., and Lippard, S. J. (1991) X-ray absorption, Mossbauer, and EPR studies of the dinuclear iron center in the hydroxylase component of methane monooxygenase. *J. Am. Chem. Soc. 113*, 9219–9235.
37. Davydov, R., Valentine, A. M., Komar-Panicucci, S., Hoffman, B. M., and Lippard, S. J. (1999) An EPR study of the dinuclear iron site in the soluble methane monooxygenase from *Methylococcus capsulatus* (Bath) reduced by one electron at 77 K: The effects of component interactions and the binding of small molecules to the diiron(III) center. *Biochemistry 38*, 4188–4197.
38. Berthold, D. A., Voevodskaya, N., Stenmark, P., Graslund, A., and Nordlund, P. (2002) EPR studies of the mitochondrial alternative oxidase. Evidence for a diiron carboxylate center. *J. Biol. Chem. 277*, 43608–43614.
39. Daiyasu, H., Osaka, K., Ishino, Y., and Toh, H. (2001) Expansion of the zinc metallo-hydrolase family of the beta-lactamase fold. *FEBS Lett. 503*, 1–6.
40. Frazao, C., Silva, G., Gomes, C. M., Matias, P., Coelho, R., Sieker, L., Macedo, S., Liu, M. Y., Oliveira, S., Teixeira, M., Xavier, A. V., Rodrigues-Pousada, C., Carrondo, M. A., and Le Gall, J. (2000) Structure of a dioxygen reduction enzyme from *Desulfovibrio gigas*. *Nat. Struct. Biol. 7*, 1041–1045.
41. Silaghi-Dumitrescu, R., Kurtz, D. M., Jr., Ljungdahl, L. G., and Lanzilotta, W. N. (2005) X-ray crystal structures of *Moorella thermoacetica* FprA. Novel diiron site structure and mechanistic insights into a scavenging nitric oxide reductase. *Biochemistry 44*, 6492–6501.
42. Seedorf, H., Hagemeier, C. H., Shima, S., Thauer, R. K., Warkentin, E., and Ermler, U. (2007) Structure of coenzyme F420H2 oxidase (FprA), a di-iron flavoprotein from methanogenic Archaea catalyzing the reduction of O_2 to H_2O. *FEBS J. 274*, 1588–1599.
43. Guddat, L. W., McAlpine, A. S., Hume, D., Hamilton, S., de Jersey, J., and Martin, J. L. (1999) Crystal structure of mammalian purple acid phosphatase. *Structure 7*, 757–767.
44. Garau, G., Lemaire, D., Vernet, T., Dideberg, O., and Di Guilmi, A. M. (2005) Crystal structure of phosphorylcholine esterase domain of the virulence factor choline-binding protein E from *Streptococcus pneumoniae*: New structural features among the metallo-beta-lactamase superfamily. *J. Biol. Chem. 280*, 28591–28600.
45. Vicente, J. B., Carrondo, M. A., Teixeira, M., and Frazao, C. (2008) Structural studies on flavodiiron proteins. *Methods Enzymol. 437*, 3–19.
46. Thomas, P. W., Stone, E. M., Costello, A. L., Tierney, D. L., and Fast, W. (2005) The quorum-quenching lactonase from *Bacillus thuringiensis* is a metalloprotein. *Biochemistry 44*, 7559–7569.
47. Dong, Y. H., Xu, J. L., Li, X. Z., and Zhang, L. H. (2000) AiiA, an enzyme that inactivates the acylhomoserine lactone quorum-sensing signal and attenuates the virulence of *Erwinia carotovora*. *Proc. Natl. Acad. Sci. U.S.A. 97*, 3526–3531.
48. Liu, D., Momb, J., Thomas, P. W., Moulin, A., Petsko, G. A., Fast, W., and Ringe, D. (2008) Mechanism of the quorum-quenching lactonase (AiiA) from *Bacillus thuringiensis*. 1. Product-bound structures. *Biochemistry 47*, 7706–7714.
49. Jackson, C. J., Carr, P. D., Kim, H. K., Liu, J. W., Herrald, P., Mitic, N., Schenk, G., Smith, C. A., and Ollis, D. L. (2006) Anomalous scattering analysis of *Agrobacterium radiobacter* phosphotriesterase: The prominent role of iron in the heterobinuclear active site. *Biochem. J. 397*, 501–508.
50. Lindqvist, Y., Johansson, E., Kaija, H., Vihko, P., and Schneider, G. (1999) Three-dimensional structure of a mammalian purple acid phosphatase at 2.2 Å resolution with a mu-(hydr)oxo bridged di-iron center. *J. Mol. Biol. 291*, 135–147.
51. Twitchett, M. B., Schenk, G., Aquino, M. A., Yiu, D. T., Lau, T. C., and Sykes, A. G. (2002) Reactivity of M(II) metal-substituted derivatives of pig purple acid phosphatase (uteroferrin) with phosphate. *Inorg. Chem. 41*, 5787–5794.
52. Dosselaere, F., and Vanderleyden, J. (2001) A metabolic node in action: Chorismate-utilizing enzymes in microorganisms. *Crit. Rev. Microbiol. 27*, 75–131.
53. Herrmann, K. M. (1995) The shikimate pathway as an entry to aromatic secondary metabolism. *Plant Physiol. 107*, 7–12.
54. Dominski, Z. (2007) Nucleases of the metallo-beta-lactamase family and their role in DNA and RNA metabolism. *Crit. Rev. Biochem. Mol. Biol. 42*, 67–93.
55. Mitic, N., Smith, S. J., Neves, A., Guddat, L. W., Gahan, L. R., and Schenk, G. (2006) The catalytic mechanisms of binuclear metallohydrolases. *Chem. Rev. 106*, 3338–3363.
56. DeLano, W. L. (2002) in The PyMOL User's Manual, DeLano Scientific, San Carlos, CA.
57. Petrek, M., Otyepka, M., Banas, P., Kosinova, P., Koca, J., and Damborsky, J. (2006) CAVER: a new tool to explore routes from protein clefts, pockets and cavities. *BMC Bioinf. 7*, 316.